Improving estimation of intracellular hyperpolarized 1-^{13}C-pyruvate kinetics by co-injection of gadolinium contrast agent

M. Smith[1], E. Peterson[2], J. Gordon[1], K. Wang[1], I. Rowland[3], and S. Fain[1,3]
[1]Medical Physics, University of Wisconsin, Madison, WI, United States, [2]Biomedical Engineering, University of Wisconsin, Madison, WI, United States, [3]Radiology, University of Wisconsin, Madison, WI, United States

INTRODUCTION Hyperpolarized (HP) ^{13}C-labeled pyruvate studies with MR have been used to observe the dynamic ^{13}C label transfer to other metabolites. It has been shown that rate constants estimated by kinetic modeling can indicate a response to treatment [1,2]. These rates, however, reflect not only chemical exchange but membrane transport and pyruvate delivery to the region of interest. In cell culture, Harris et al. [3] flushed (removed) the extracellular space with a bioreactor perfusion system leaving adherent cells and their intracellular compartment intact. Results indicated that label flux in their T47D cells is chiefly determined by cellular uptake via monocarboxylate transporters (MCTs). Instead of eliminating the extracellular pyruvate supply in order to separate membrane transport dynamics and i ntracellular chemical exchange, we present an alternative technique to provide a predictable contrast to the non-intracellular compartments by following the injection of HP [1-^{13}C]-pyruvate with an injection of a T_1-shortening contrast agent (CA). In this work, we first investigate the limitations of kinetic modeling of the *in-vivo* ^{13}C label dynamics using a widely used two-site exchange model [1]. We then provide a kinetic model that distinguishes the intracellular space by utilizing this contrast.

METHODS *Simulations:* A five-compartment kinetic model that separates intracellular and extracellular comp onents was used to create kinetic curves from these compartments (**Fig 1a**). Model param eter values were selected to mimic the total pyruvate and lactate signal typically seen using HP ^{13}C MR spectroscopy techniques. This 'truth' dataset was then fitted with the two-site exchange model (**Fig 1b**) commonly used in the literature [1]. Next, a simplified four-compartment model (**Fig 1c**) was used to simulate signal dynamics with injection of a T_1-shortening contrast agent (CA) that is restricted from, and therefore provides contrast to, the intracellular space. The four-compartment model was not applied to the simulated data because no contrast was simulated. *Experiment:* A mouse (32 g) was imaged with a custom dual-tuned ^{1}H/^{13}C volume coil in a 4.7T small-bore MRI. Spectra were obtained using a global pulse and acquire spectroscopy sequence after a HP ^{13}C-pyruvate injection. A T_1 shortening CA (Omniscan, Novation, Irving, TX, USA, 0.5mmol/kg, r1=0.23 $mM^{-1}s^{-1}$ for ^{13}C-pyruvate at 7T) was injected 20 seconds after the end of the pyruvate injection.

RESULTS The two-site exchange model (**Fig 1b**) estimates label transfer rates that reflect not only chemical exchange but membrane transport and pyruvate delivery to the region of interest. It is clear in the simulation results (**Fig 2**) that the desired physiological rates are inaccessible via the current methodology. **Fig 3** displays the simulated dynamic signals from the four-compartment model (**Fig 1c**) including the effect of the CA. Notably, a dramatic increase in the signal decay rate is evident after the CA arrival within the extracellular compartments (P_e, L_e). **Fig 4a** shows agreement between predicted (lines) and experimental *in-vivo* results (circles). A split pyruvate peak (**Fig 4b**) was present due to the bulk magnetic susceptibility of the largely vascular component (inferior vena cava) along the magnetic field [4]. Included in **Fig 4a**, these two resonances (triangles and squares) provide a unique visualization of the localized CA effect on different compartments.

DISCUSSION Simulation results demonstrate inadequate compartmental distinction using current kinetic modeling methods and requires alternative strategies to accurately estimate both membrane transport and intracellular chemical exchange. Injection of a T_1-shortening agent following a ^{13}C-pyruvate injection can not only be a technique to provide contrast to the intracellular signal *in-vivo*, but can provide perfusion and vascularity information using the dynamic ^{1}H signal if acquired simultaneously [5]. Other techniques to provide contrast between functional compartments include suppression of flowing spins in the vasculature using stimulated echoes [6], diffusion weighted gradients, or frequency shift agents [7]. Future work will investigate how sensitive the proposed technique is to model parameters and different concentrations and relaxivities of CA.

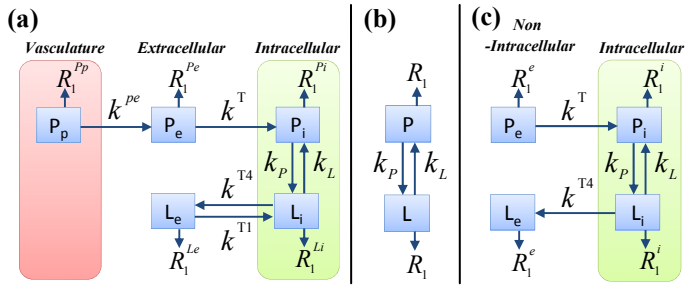

Figure 1. (a) Five-compartment model used to generate data that emulates physiological processes. (b) Two-site exchange model [1]. (c) Proposed simplified four-compartment model used to simulate signal dynamics in the presence of a CA restricted to non-intracellular compartments.

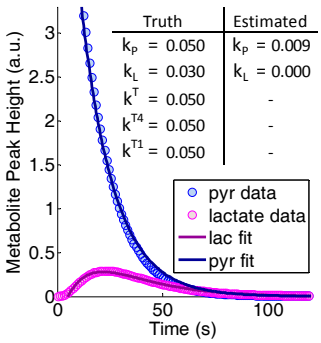

Figure 2. Data generated with the five-site exchange model (Fig 1a) fit with two-site exchange model (Fig 1b) demonstrating an inadequate representation of the ^{13}C label dynamics.

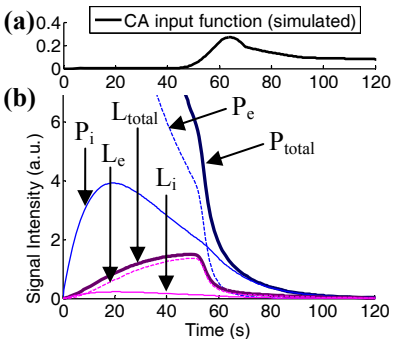

Figure 3. (a) Input function used for simulated effect of CA. (b) Compartment (Fig 1c) dynamics which demonstrates that the extracellular component decays much more rapidly than the intracellular component, providing a contrast between the two compartments.

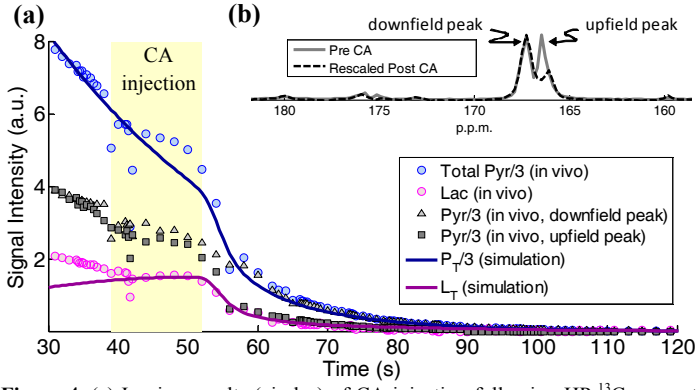

Figure 4. (a) In-vivo results (circles) of CA injection following HP ^{13}C-pyruvate injection shows agreement with simulated signal (lines). The increased relaxivity caused by the CA could help in extracting the intracellular ^{13}C label transfer. (b) Two pyruvate resonances caused by bulk susceptibility allows visualization of pyruvate from two different regions and their respective response to the CA shown as triangles and squares in (a).

References [1] Day et al., Nat Med, 2007; 13(11):1382-7. [2] Zierhut et al., J Magn Reson, 2010; 202(1):85-92. [3] Harris et al., Proc Natl Acad Sci USA, 2009; 106(43):18131-6. [4] Szczepaniak et al., MRM, 2002; 47:607–610. [5] Peterson et al., Proc. ISMRM, 2010. 1020. [6] Larson et al., Proc. ISMRM, 2010. 375. [7] Weidensteiner et al., MRM, 2002; 48:89–96.
Acknowledgements NIH/NCI 5 T32 CA009206-28, GE Healthcare